

Oxidized multiwalled carbon nanotubes as adsorbent for the removal of manganese from aqueous solution

Pandian Ganesan · Ramakrishnan Kamaraj ·
Ganapathy Sozhan · Subramanyan Vasudevan

Received: 7 March 2012 / Accepted: 10 April 2012 / Published online: 5 May 2012
© Springer-Verlag 2012

Abstract A batch adsorption process was applied to investigate the removal of manganese from aqueous solution by oxidized multiwalled carbon nanotubes (MWCNTs). In doing so, the thermodynamic, adsorption isotherm, and kinetic studies were also carried out. MWCNT with 5–10-nm outer diameter, surface area of 40–600 m²/g, and purity above 95 % was used as an adsorbent. A systematic study of the adsorption process was performed by varying pH, ionic strength, and temperature. Manganese-adsorbed MWCNT was characterized by Raman, FTIR, X-ray diffraction, XPS, SEM, and TEM. The adsorption efficiency could reach 96.82 %, suggesting that MWCNT is an excellent adsorbent for manganese removal from water. The results indicate that second-order kinetics model was well suitable to model the kinetic adsorption of manganese. Equilibrium data were well described by the typical Langmuir adsorption isotherm. Thermodynamic studies revealed that the adsorption reaction was spontaneous and endothermic process. The experimental results showed that MWCNT is an excellent manganese adsorbent. The MWCNTs removed the manganese present in the water and reduced it to a permissible level making it drinkable.

Keywords MWCNT · Manganese · Adsorption · Isotherm · Kinetics · Thermodynamics

Introduction

Manganese is the second most abundant metal in nature (Dabeka et al. 2002). It is an essential metal for the human system and many enzymes are activated by manganese. Manganese has a variety of applications in ceramics, primary cells (dry battery), and electrical coils. Manganese is also used in alloying element of many alloys. It is present in the atmosphere as suspended particulates resulting from industrial emission, soil erosion, volcanic emissions, and the burning of MMT-containing petrol (WHO 2004). The manganese contaminant in groundwater affects the intelligent quotient of children (Dabeka et al. 2002). The neurotoxic disease like Parkinsonism is caused by the manganese over intake (Erikson et al. 2007). The prolonged over intake potentially affects the central nervous system and lungs. These manganese contaminants in the groundwater cause a disease called manganism, diseases of disturbed speech with poor prognosis, and also bronchitis and pneumonia (US EPA report). The World Health Organization prescribed permissible limit for the manganese in the groundwater is 0.05 mg/L (WHO 2004).

The common methods for removing toxic metals from water include electro dialysis, chemical and electrocoagulation, reverse osmosis, coprecipitation, complexation, solvent extraction, ion exchange, and adsorption (Bedow et al. 2008; Nogawa et al. 2004; Friberg 1983; Vasudevan et al. 2008, 2009, 2010a, b, c, d, e; Vasudevan and Lakshmi 2011, 2012a, b; Sekar et al. 2004; Youssef et al. 2004; Gupta et al. 1997a, b, 1998, 2000, 2001, 2002; Gupta and Sharma 2003; Gupta and Ali 2004; Gupta et al. 2006a, b, c, d, 2007a, b, c, d, e; Gupta and Rastogi 2008a, b, c, d; Gupta and Ali 2008f, e; Gupta et al. 2009a, b, c, d, e, f, g; Gupta and Rastogi 2010; Gupta et al. 2012; Ali and Gupta 2007; Ali 2010; Jain et al. 1995a, b, 1997a, b; Srivastava et al. 1995, 1997; Goyal et al.

Responsible editor: Vinod Kumar Gupta

P. Ganesan · R. Kamaraj · G. Sozhan · S. Vasudevan (✉)
CSIR-Central Electrochemical Research Institute,
Karaikudi 630 006, India
e-mail: vasudevan65@gmail.com

2007a, b; Saleh and Gupta 2011). Physical methods like ion exchange, reverse osmosis, and electro dialysis have proven to be either too expensive or inefficient to remove manganese from water. At present, chemical treatments are not used due to disadvantages like high costs of maintenance, problems of sludge handling and its disposal, and neutralization of effluent (Mollah et al. 2001; Mouedhen et al. 2008; Melnik et al. 1999). Among these treatment methods, adsorption process is more advantageous due to low cost and high treatment efficiency.

Carbon nanotubes (CNTs) have large surface area, high mechanical strength, and remarkable electrical conductivities which have been indicated for their tremendous potential for different applications. CNTs are classified into two categories, viz. single-walled carbon nanotubes and multi-walled carbon nanotubes (MWCNTs). The application of MWCNT as an adsorbent to remove organic and inorganic pollutants has been studied intensively (Wang et al. 2005; Fugetsu et al. 2004; Chen and Wang 2006; Yang et al. 2006), and the results indicate that MWCNTs are suitable candidate for water treatment. However, the adsorption of manganese to MWCNT is still scarce. The objectives of this study include: (1) to investigate the adsorption kinetics of manganese on the MWCNT; (2) to study the effects of pH, ionic strength, and foreign ions on manganese sorption on the MWCNT; (3) to study the adsorption isotherms by using Langmuir and Freundlich models; and (4) to calculate the thermodynamic parameters for the adsorption of manganese at different temperatures.

Materials and methods

Materials

MWCNTs were purchased from Aldrich, with 5–10-nm outer diameter, surface area of 40–600 m²/g, and purity above 95 %.

Preparation of purified MWCNT and characterization

Ten grams of raw MWCNT was soaked in 50 mL of 8 mol/L of HNO₃ for 12 h at room temperature. Then, the solution was filtered through a 0.45- μ m membrane filter and the MWCNTs were washed with Milli-Q water until the neutral pH. Then, the MWCNTs were refluxed with 8 mol/L nitric acid solution at about 125 °C for 2 h, filtered, and then washed with deionized water until neutral pH. Such prepared MWCNT was dried overnight in an oven at 80 °C and then calcined at 450 °C for 4 h to completely remove amorphous carbon and nitrate ions.

The morphology and structure of MWCNT were characterized by scanning electron microscope (SEM) (Hitachi model s-3000h, Japan) and by transmission electron microscopy

(TEM) (Hitachi 800). The Fourier transform infrared spectroscopy (FTIR) spectrum of MWCNT was recorded with a FTIR spectrometer (Nexus 670, USA). Raman spectroscopy was performed with a Renishaw InVia Laser Raman Microscope. The X-ray diffraction (XRD) pattern of MWCNT was analyzed using an X'per PRO X-ray diffractometer (PANalytical, USA). The X-ray photoelectron spectroscopy (XPS) spectra were recorded on powders with a thermo ESCALAB 250 spectrometer using an AlK α monochromator source and a multidetection analyzer, under a 10–8-Pa residual pressure.

Batch mode adsorption experiment

Batch adsorption experiments were performed using 100-mL glass bottles with the addition of 50 mg of MWCNT and 75 ml of manganese (Mn(NO₃)₂) solution of concentration from 0.25 to 2.0 mg/l. The glass bottles were sealed with Teflon and then were placed on a shaker. The adsorption experiments were carried out at 180 rpm for 12 h (25 °C). The temperature of the manganese solution has been controlled to the desired value with a variation of ± 2 K by adjusting the rate of flow of thermostatically controlled water through an external glass-cooling spiral. All chemicals were purchased in analytical purity and used in the experiments directly without any further purification. All solutions were prepared using Milli-Q water.

Analytical method

All the ions, viz. manganese, sulfate, nitrate, fluoride, and phosphate were measured using an ion chromatograph (Metrohm AG, Herisau, Switzerland) equipped with a Dual 3 column (250 \times 4 mm), an RP guard column, and a conductivity detector. NaOH (5 mM) served as the eluent and sulfuric acid (2.0 mM) as the regenerant in the chromatogram analysis.

Theory

Kinetic modeling

In order to investigate the mechanisms of the manganese adsorption process, two different kinetic models (Gupta and Sharma 2003), the pseudo-first-order model and pseudo-second-order model, were applied to describe the kinetics of the manganese adsorption onto MWCNT.

First-order Lagergren model

The first-order rate equation of the Lagergren model is one of the most widely used expressions describing the

adsorption of solute from a solution. The first-order Lagergren model is generally expressed as follows (Sharma and Bhattacharyya 2004):

$$dq_t/dt = k_1(q_e - q_t) \tag{1}$$

where q_e and q_t are the adsorption capacities at equilibrium and at time t (in minutes), respectively, and k_1 (in minutes) is the rate constant of first-order adsorption. The integrated form of the above equation with the boundary conditions $t=0$ to >0 ($q=0$ to >0) is rearranged to obtain the following time-dependent function:

$$\log(q_e - q_t) = \log(q_e) - k_1t/2.303. \tag{2}$$

Second-order Lagergren model

The Lagergren second-order kinetic model is expressed as (Ho and McKay 1998):

$$dq_t/dt = k_2(q_e - q_t)^2 \tag{3}$$

where k_2 is the rate constant of second-order adsorption. The integrated form of Eq. (3) with the boundary condition $t=0$ to >0 ($q=0$ to >0) is:

$$1/(q_e - q_t) = 1/q_e + k_2t. \tag{4}$$

Equation (4) can be rearranged and linearized as:

$$t/q_t = 1/k_2q_e^2 + t/q_e \tag{5}$$

where q_e and q_t are the amount of manganese adsorbed on MWCNT (in milligrams per gram) at equilibrium and at time t (in minutes), respectively, and k_2 is the rate constant for the second-order kinetic model.

Isotherm modeling

In order to identify the mechanism of the adsorption process, it is important to establish the most appropriate correlation for the equilibrium curves. In this study, two adsorption isotherms, Langmuir and Freundlich, were applied to establish the relationship between the amounts of manganese adsorbed onto the MWCNT and its equilibrium concentration in the aqueous solution containing manganese.

Freundlich isotherm

The Freundlich adsorption isotherm typically fits the experimental data over a wide range of concentrations. This empirical model includes considerations of surface heterogeneity and exponential distribution of the active sites and their energies. The isotherm is adopted to describe reversible adsorption and is not restricted to monolayer formation. The linearized in logarithmic form and the Freundlich constants

can be expressed as (Freundlich 1907):

$$\log q_e = \log k_f + n \log C_e \tag{6}$$

where k_f is the Freundlich constant related to adsorption capacity, n is the energy or intensity of adsorption, C_e is the equilibrium concentration of manganese (in milligrams per liter).

Langmuir isotherm

The Langmuir model was originally developed to represent chemisorption at a set of well-defined localized adsorption sites with the same adsorption energy, independent of the surface coverage, and with no interaction between adsorbed molecules. This model assumes a monolayer deposition on a surface with a finite number of identical sites (McKay et al. 1982). It is well known that the Langmuir equation is valid for a homogeneous surface. The linearized form of Langmuir adsorption isotherm model is:

$$C_e/q_e = 1/q_m b + C_e/q_m \tag{7}$$

where q_e is the amount adsorbed at equilibrium concentration C_e , q_m is the Langmuir constant representing maximum monolayer adsorption capacity, and b is the Langmuir constant related to energy of adsorption. The essential characteristics of the Langmuir isotherm can be expressed as the dimensionless constant R_L .

$$R_L = 1/(1 + bC_o) \tag{8}$$

where R_L is the equilibrium constant that indicates the type of adsorption, b , is the Langmuir constant (Langmuir 1918). C_o is various concentrations of manganese solution. The R_L values between 0 and 1 indicate the favorable adsorption.

Thermodynamic parameters

To understand the effect of temperature on the adsorption process, thermodynamic parameters should be determined at various temperatures (Golder et al. 2006). The energy of activation for adsorption of manganese can be determined by the second-order rate constant expressed in Arrhenius form.

$$\ln k_2 = \ln k_o - E/RT \tag{9}$$

where k_o is the constant of the equation (in grams per milligram per minute), E is the energy of activation (in joules per mole), R is the gas constant ($8.314 \text{ Jmol}^{-1} \text{ K}^{-1}$), and T is the temperature in kelvin. The free energy change is obtained using the following relationship:

$$\Delta G = -RT \ln K_c \tag{10}$$

where ΔG is the free energy (in kilojoules per mole), K_c is the

equilibrium constant, R is the gas constant, and T is the temperature in kelvin. Other thermodynamic parameters such as entropy change (ΔS) and enthalpy change (ΔH) were determined using van't Hoff equation:

$$\ln K_c = \frac{\Delta S}{R} - \frac{\Delta H}{RT}. \quad (11)$$

Pore diffusion coefficient (D)

The diffusion coefficient (D) for intraparticle transport of manganese species into the adsorbent particles has been calculated at different temperature by:

$$t_{1/2} = 0.03x r_o^2 / D \quad (12)$$

where $t_{1/2}$ is the time of half adsorption (in seconds), r_o is the radius of the adsorbent particle (in centimeters), D is the diffusion coefficient in square centimeter per second (Golder et al. 2006).

Results and discussion

Characterizations of MWCNT

The Raman spectrum of MWCNT in Fig. 1 is composed of two characteristic peaks. The peak near $1,350 \text{ cm}^{-1}$ is the D-band corresponding to the disordered sp^2 -hybridized carbon atoms of MWCNT, while the peak near $1,580 \text{ cm}^{-1}$ is the G-band corresponding to the structural integrity of sp^2 -hybridized carbon atoms of MWCNT. Together, these bands can be used to determine the extent of carbon-containing defects. As can be seen, unoxidized MWCNTs (ID/IG=0.85) have a higher ID/IG ratio (the intensity ratio of D-band to G-band) than the MWCNT (ID/IG=0.79), which indicates that the MWCNTs contain more amorphous carbon and multishell

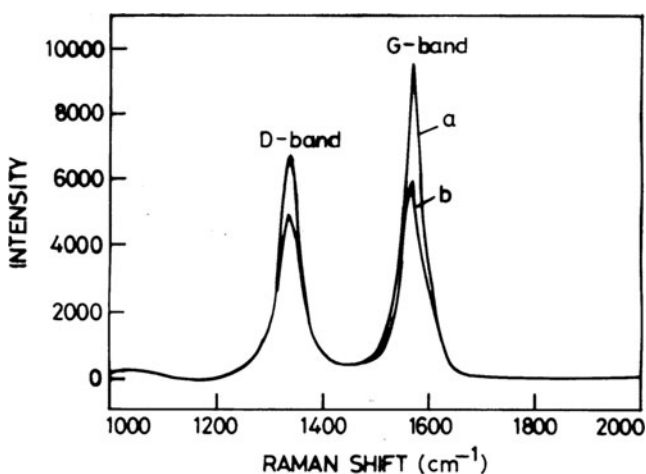


Fig. 1 Raman spectra of *a* MWCNT and *b* MWCNT (unoxidized)

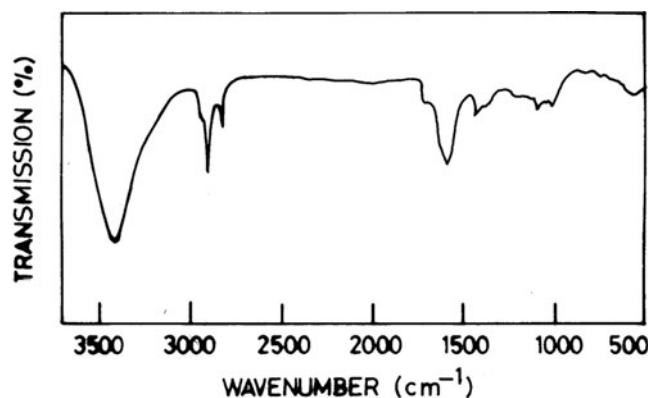


Fig. 2 Fourier transformed infrared spectra of MWCNT

sp^2 -hybridized carbon nanoparticles that can encapsulate residual metal catalysts. In other words, the raw MWCNTs have less crystalline graphitic structures.

The FTIR measurements were performed in order to verify the formation of oxygen-containing functional groups after oxidation. Figure 2 shows the FTIR spectra of O-MWCNT. The FTIR spectra indicate that the acid treatment process introduces many functional groups on the surfaces of MWCNT: carbonyl groups ($1,400 \text{ cm}^{-1}$), carboxyl groups ($1,650 \text{ cm}^{-1}$), and hydroxyl groups ($3,500 \text{ cm}^{-1}$). These functional groups are produced abundantly on the external and internal surface of MWCNT, which increase the surface polarity and further alter the surface charges.

Figure 3 shows the XRD pattern of the MWCNT structure. The most intense peaks of MWCNT correspond to the (0 0 2) and (1 0 0) reflections.

Figure 4 shows the high-resolution XPS spectra of the sample around 532.5 eV . With reference to the XPS studies of MWCNT, the experimental data show that functional groups present on the surface of MWCNT: carboxyl oxygen [$-\text{O}-\text{C}=\text{O}$ (H), 533.6 eV] and carbonyl oxygen ($=\text{C}=\text{O}$, 530.7 eV).

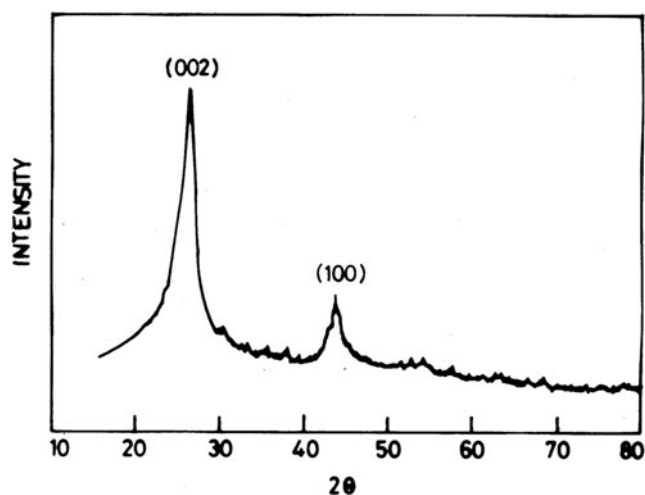


Fig. 3 XRD pattern of MWCNT

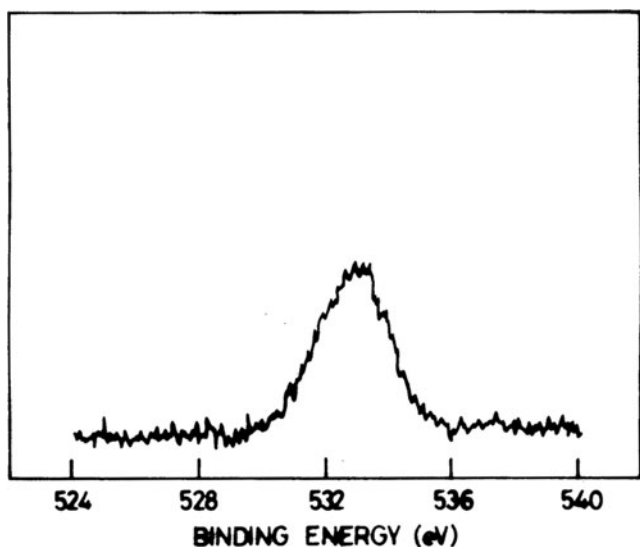


Fig. 4 XPS spectra of MWCNT

The morphology of MWCNT was examined by using SEM and TEM. From the SEM, it is found that the MWCNTs have very smooth surfaces and are about 100–200 nm in diameter and several micrometers in length (Fig. 5). Figure 6 shows the TEM of the MWCNT after adsorption experiments. The black dots show the adsorption on manganese on MWCNT.

Effect of pH and competing anions

The pH value plays an important role with respect to the adsorption of particular ions on MWCNT. When pH of the solution is higher than pH_{PZC} , the negative charge on the surface provides electrostatic interactions that are favorable for adsorbing cationic species. The decrease of pH leads to neutralization of surface charge, thus, the adsorption of cations should decrease. To examine this effect, a series of

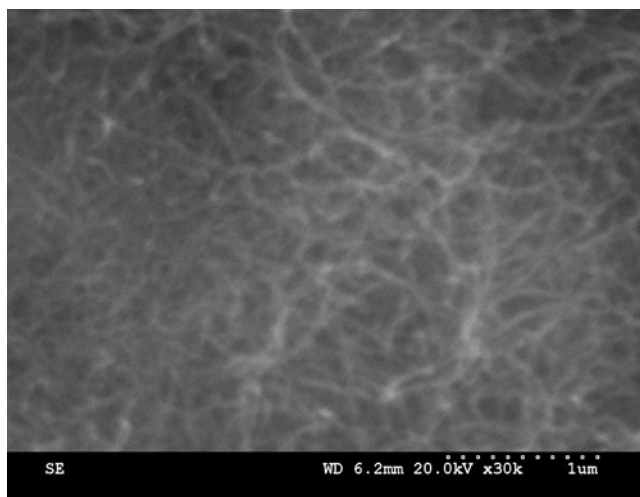


Fig. 5 SEM image of MWCNT

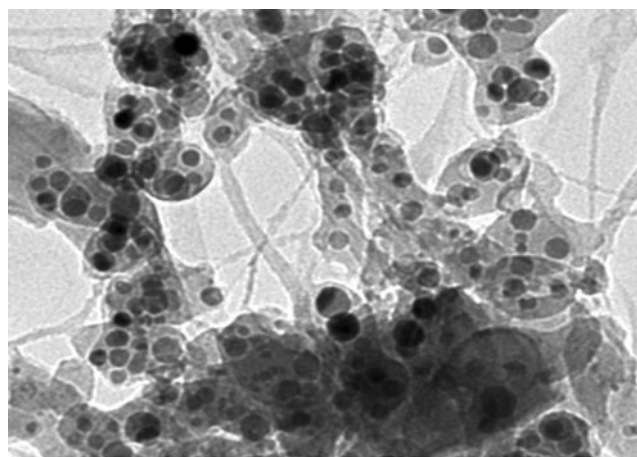


Fig. 6 TEM image of MWCNT after adsorption

experiments were carried out using 2 mg/L manganese-containing solutions, with an initial pH varying in the range from 2 to 12.

The obtained results indicate that the adsorption of manganese increased with the increase of pH from 2 to 12. The low adsorption that took place in acidic region can be attributed in part to competition between H^+ and manganese ions on the same sites. Furthermore, the charge of MWCNT surface becomes more negative with the increase of pH, which causes electrostatic interactions and thus results in higher adsorption of metal species.

The impact of various anions (commonly present in water) including fluoride (F^-), nitrate (NO_3^-), sulfate (SO_4^{2-}), and phosphate (PO_4^{3-}) on manganese removal by MWCNT was investigated at 2.0 mg/L of initial manganese concentration. Anions present in the manganese solutions are likely to limit the manganese removal efficiency. In the presence of nitrate,

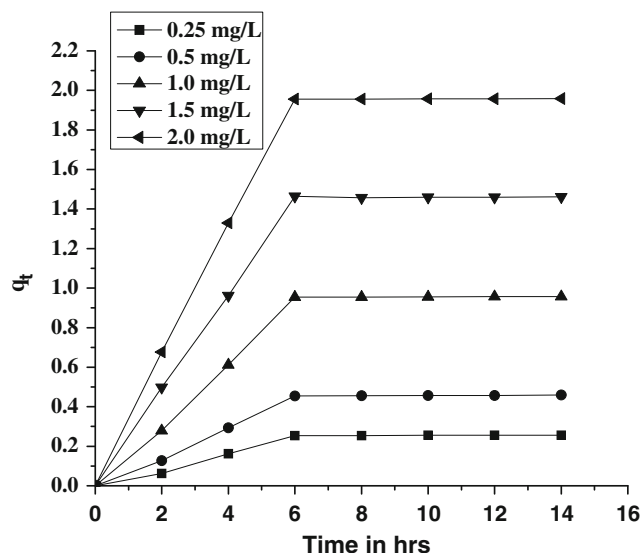


Fig. 7 Effect of electrolysis time and amount of manganese adsorbed. Conditions: pH, 7.0 and temperature, 303 K

Table 1 Amount of manganese adsorbed for the various temperatures (303–343 K) at various concentrations (0.25–2.0 mg/L)

Temperature (K)	Amount of manganese adsorbed for different concentrations (mg/L)				
	0.25	0.5	1.0	1.5	2.0
303	0.202	0.456	0.954	1.453	1.952
313	0.204	0.458	0.956	1.456	1.953
323	0.207	0.461	0.959	1.459	1.954
333	0.209	0.463	0.962	1.461	1.955
343	0.210	0.465	0.963	1.463	1.956

the removal efficiency of manganese was 96.62, 96.2, and 96.0 % for the concentrations of 20, 50, and 100 mg/L, respectively; while in case of other anions (fluoride, sulfate, and phosphate), the removal efficiency of perchlorate was 96.3, 96.1, and 96.0 % for the concentrations of 20, 50, and 100 mg/L, respectively. There was no significant change in the removal efficiency of manganese under the investigated competing anions.

Effect of concentration

In order to evaluate the effect of initial manganese concentration, experiments were conducted at varying initial concentrations from 0.25 to 2.0 mg/L. From Fig. 7, it is clear that the adsorption of manganese is increased with an increase concentration remains constant after the equilibrium time. The equilibrium time was 354 min for all of the concentrations studied (0.25–2.0 mg/L). Table 1 reveals the increase in adsorption with an increase in manganese concentration at different temperature at equilibrium time.

Kinetic modeling

In order to establish the kinetic of manganese adsorption, adsorption kinetics of MWCNT was investigated by using first-order and second-order kinetic models. In the present investigation, two kinetic models, namely pseudo-first-order and pseudo-second-order, were tested to obtain rate constants, equilibrium adsorption capacity, and adsorption mechanism at various temperatures (303–343 K).

Table 2 Comparison between the experimental and calculated q_e values at different temperature for first- and second-order adsorption isotherm for manganese concentration of 2.0 mg/L

Temperature (K)	q_e (exp)	First-order adsorption			Second-order adsorption		
		q_e (cal)	$k_1 \times 10^4$ (min/mg)	R^2	q_e (cal)	$k_2 \times 10^4$ (min/mg)	R^2
303	1.952	22.14	-0.0074	0.7658	1.950	0.0657	0.9989
313	1.953	25.23	-0.0071	0.8032	1.952	0.0661	0.9995
323	1.954	29.14	-0.0069	0.7991	1.951	0.0665	0.9985
333	1.955	30.01	-0.0073	0.6654	1.950	0.0671	0.9985
343	1.956	31.04	-0.0075	0.6847	1.952	0.0673	0.9987

First-order Lagergren model

The experimental data were analyzed initially with first-order Lagergren model. The plot of $\log(q_e - q_t)$ versus t should give the linear relationship, from which k_1 and q_e can be determined by the slope and intercept, respectively, from Eq. (2). The computed results are presented in Table 2. In all the adsorption experiments, the results show that the theoretical q_e (cal) value does not agree to the experimental q_e (exp) values with poor correlation coefficient. So, further experimental data were fitted with second-order Lagergren model.

Second-order Lagergren model

The kinetic data were fitted to the second-order Lagergren model using Eq. (5). The equilibrium adsorption capacity, q_e (cal), and k_2 were determined from the slope and intercept of plot of t/q_t versus t (Fig. 8) and were compiled in Table 2. The plots were found to be linear with good correlation coefficients. The theoretical q_e (cal) values agree well to the experimental q_e (exp) values at all concentrations studied. This implies that the second-order model is in good agreement with experimental data and can be used to favorably explain the manganese adsorption on MWCNT.

Table 2 depicts the computed results obtained from first- and second-order models. From the results, it is observed that the correlation coefficients for the first-order kinetic model were relatively lower than those obtained for the second-order kinetic model for the different concentrations.

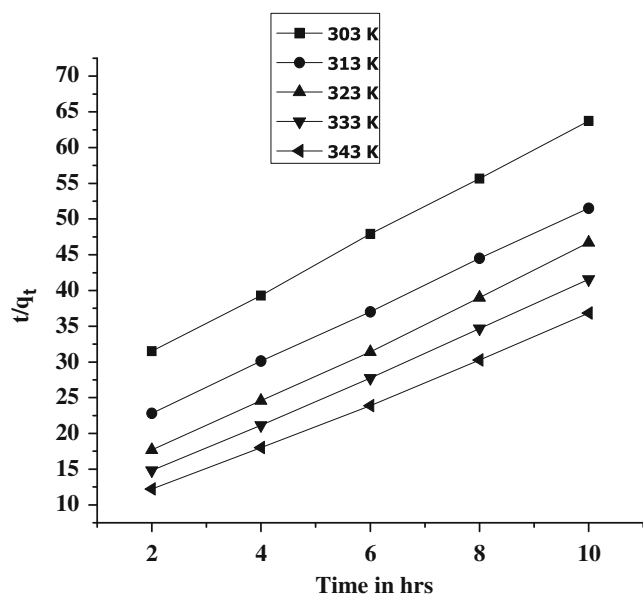


Fig. 8 Second-order kinetic model plot for the adsorption of manganese. Conditions: concentration, 2 mg/L; temperature, 303–343 K

These results indicate that the second-order kinetic model can be applied suitably to predict the manganese adsorption process onto MWCNTs.

Isotherm modeling

Freundlich isotherm

In testing the isotherm, the manganese concentration used was from 0.25 to 2.0 mg/L. The adsorption data are plotted as $\log q_e$ versus $\log C_e$ by Eq. (6) should result in a straight line with slope n and intercept k_f . The intercept and the slope are indicators of adsorption capacity and adsorption intensity, respectively. The value of n falling in the range of 1–10 indicates favorable sorption. The k_f and n values were listed in Table 3 for each concentration. It has been reported that values of n lying between 0 and 10 indicate favorable adsorption. From the analysis of the results, it is found that

the Freundlich plots fit satisfactorily with the experimental data obtained in the present study.

Langmuir isotherm

Langmuir isotherm was tested from Eq. (7). The plots of $1/q_e$ as a function of $1/C_e$ for the adsorption of manganese on MWCNT are shown in Fig. 9. The plots were found linear with good correlation coefficients (>0.99) indicating the applicability of Langmuir model in the present study. The values of monolayer capacity (q_m) and Langmuir constant (b) is given in Table 3. The values of q_m calculated by the Langmuir isotherm were all close to experimental values at given experimental conditions. These facts suggest that manganese is adsorbed in the form of monolayer coverage on the surface of the adsorbent.

The applicability of the two isotherm equations was compared using the correlation coefficient (R^2). The correlation coefficient values of Freundlich and Langmuir isotherm models are presented in Table 3. The values of R^2 are found to be >0.9 for both isotherms. However, based on the R^2 values, the Langmuir isotherm model provided a better fit compared to the Freundlich isotherm model. This suggests the adsorption of manganese by MWCNTs is apparently with monolayer coverage of adsorbed molecules. The dimensionless constant R_L was calculated from Eq. (8). The R_L values were found to be between 0 and 1 for all the concentration of manganese studied.

Thermodynamic parameters

Figure 10 shows that the rate constants vary with temperature according to Eq. (10). The activation energy (0.6712 kJ/mol) is calculated from slope of the fitted equation. The free energy change is obtained from Eq. (10). The K_c and ΔG values are presented in Table 4. From the table, it is found that the negative value of ΔG indicates the spontaneous nature of adsorption. The enthalpy change ($\Delta H=3.143$ kJ/mol) and entropy change ($\Delta S=0.7174$ J/mol K) were obtained from the slope and intercept of the van't Hoff linear plots of $\ln k_c$

Table 3 Constant parameters and correlation coefficient calculated for different adsorption isotherm models at different temperature for manganese adsorption at 2.0 mg/L at pH 7

Isotherm	Parameters	Temperature (K)				
		303	313	323	333	343
Freundlich	k_f (mg/g)	1.2387	1.2853	1.3269	1.3584	1.3891
	n (L/mg)	1.1260	1.1543	1.1924	1.2158	1.2574
	R^2	0.9859	0.9836	0.9872	0.9798	0.9883
Langmuir	q_m (mg/g)	3.3542	3.4157	3.4432	3.4781	3.5015
	b (L/mg)	4.3087	4.3351	3.3564	3.3714	3.3961
	R^2	0.9988	0.9978	0.9995	0.9987	0.9966
	R_L	0.6862	0.6714	0.6748	0.6715	0.6782

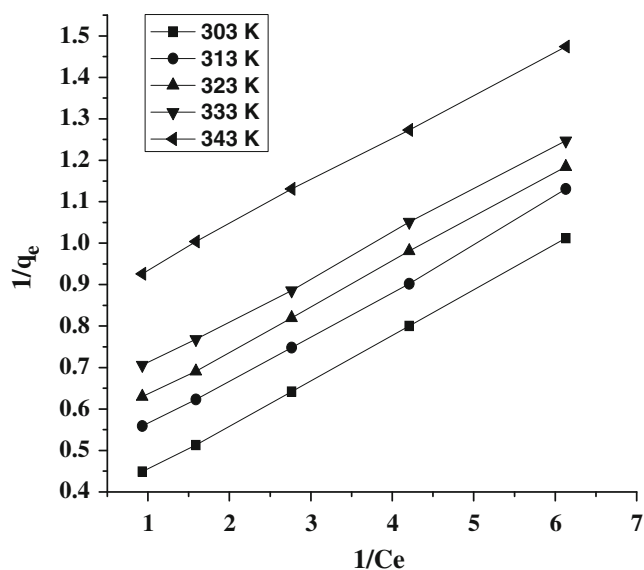


Fig. 9 Langmuir plot for adsorption of manganese. Conditions: pH of the electrolyte, 7.0; temperature, 303–343 K; and concentration, 2.0 mg/L

versus $1/T$ (Fig. 11 and Eq. 12). A positive value of enthalpy change (ΔH) indicates that the adsorption process is endothermic in nature, and the negative value of change in internal energy (ΔG) shows the spontaneous adsorption of manganese on the adsorbent. Positive values of entropy change show the increased randomness of the solution interface during the adsorption of manganese on the adsorbent (Table 4). Enhancement of adsorption capacity of MWCNT at higher temperatures may be attributed to the high porosity and or activation of the adsorbent surface and availability of more surface area due to carbon nanotubes as concentric cylinders (Guodong et al. 2010). Using Lagergren rate equation, second-order

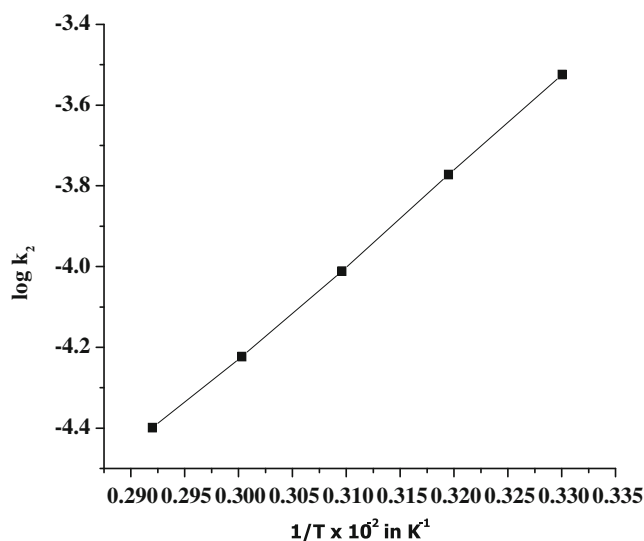


Fig. 10 Plot of $\log k_2$ and $1/T$. Condition: concentration, 2.0 mg/L

Table 4 Thermodynamic parameters for adsorption of manganese

Temperature (K)	K_c	ΔG° (J/mol)	ΔH° (kJ/mol)	ΔS° (J/mol K)
303	17.258	-222.98		
313	18.065	-224.12	3.143	0.7174
323	20.022	-232.24		
333	21.088	-239.07		
343	22.132	-240.12		

rate constants and correlation coefficient were calculated for different temperatures (303–343 K). The calculated “ q_c ” values obtained from the second-order kinetics agree with the experimental q_c values better than the first-order kinetics model, indicating adsorption following second-order kinetics.

Conclusions

In this paper, the adsorption behavior of manganese on MWCNT was investigated. The experimental results indicate that MWCNT can effectively remove manganese in an aqueous solution. The percentage of manganese removal by MWCNT can reach 96.82 %. Kinetic studies suggest that the equilibrium is achieved only within 354 min and the pseudo-second-order model is followed. The adsorption isotherms could be well fitted by the Langmuir adsorption isotherm equations. Temperature studies showed that adsorption was endothermic and spontaneous in nature. The results obtained in this work suggest that MWCNT has a potential application as an adsorbent media for removing manganese from water.

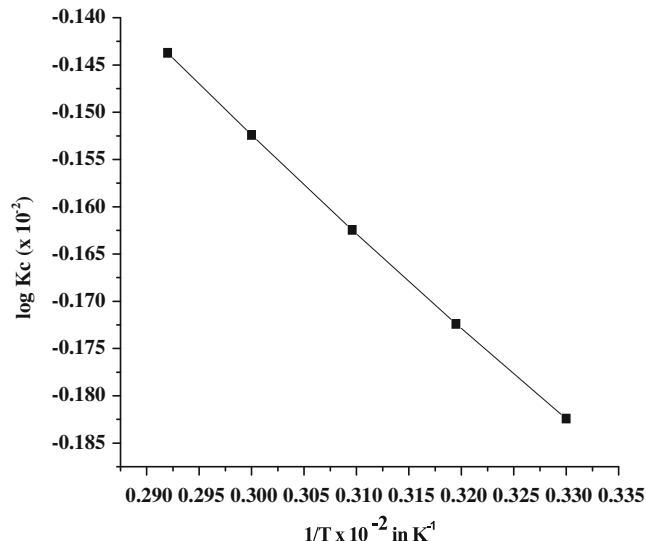


Fig. 11 Plot of $\ln K_c$ and $1/T$. Condition: concentration of 2.0 mg/L

Acknowledgments The authors wish to express their gratitude to the Director of Central Electrochemical Research Institute, Karaikudi for the publication of this paper.

References

- Ali I (2010) The quest for active carbon adsorbent substitutes: inexpensive adsorbents for toxic metal ions removal from wastewater. *Sep Purif Rev* 39:95–171
- Ali I, Gupta VK (2007) Advances in water treatment by adsorption technology. *Nat Protoc* 1:2661–2667
- Bedow K, Bekri-Abbes I, Srasra E (2008) Removal of cadmium (II) from aqueous using pure smectitic and Lewtite S100: the effects of time and metal concentration. *Desalination* 223:269–273
- Chen CL, Wang XK (2006) Adsorption of Ni(II) from aqueous solution using oxidized multi-walled carbon nanotubes. *Ind Eng Chem Res* 45:9144–9149
- Dabeka RW, Conacher HB, Lawrence JF, Newsome WH, McKenzie A, Wagner HP (2002) Survey of bottled drinking waters sold in Canada for chlorate, bromide, bromate, lead, cadmium and other trace elements. *Food Addit Contam* 19:721–732
- Erikson KM, Thompson K, Aschner J, Aschne M (2007) Manganese neurotoxicity A: focus on neonate. *Pharmacol Ther* 113:369–377
- Freundlich H (1907) Ueber die adsorption in Loesungen. *Phys Chem* 57:385–470
- Friberg L (1983) Cadmium. *Annu Rev Public Health* 4:367
- Fugetsu B, Satoh S, Shiba T, Mizutani T, Lin YB, Terui N, Nodasaka Y, Sasa K, Shimizu K, Akasaka T, Yokoyama A, Mori M, Tanaka K, Sato Y, Tohji K, Tanaka S, Nishi N, Watari F (2004) Caged multiwalled carbon nanotubes as the adsorbents for affinity-based elimination of ionic dyes. *Environ Sci Technol* 38:6890–6896
- Golder AK, Samantha AN, Ray S (2006) Removal of phosphate from aqueous solution using calcined metal hydroxides sludge waste generated from electrocoagulation. *Sep Purif Technol* 52:102–109
- Goyal RN, Gupta VK, Oyama M, Bachheti N (2007a) Gold nanoparticles modified indium tin oxide electrode for the simultaneous determination of dopamine and serotonin: application in pharmaceutical formulations and biological fluids. *Talanta* 72:976–983
- Goyal RN, Gupta VK, Oyama M, Bachheti N (2007b) Voltammetric determination of adenosine and guanosine using fullerene-C60-modified glassy carbon electrode. *Talanta* 71:1110–1117
- Guodong S, Li J, Dadong S, Jun H, Changlun C, Yixue C, Xiangke W (2010) Adsorption of copper(II) on multiwalled carbon nanotubes in the absence and presence of humic or fulvic acids. *J Hazard Mater* 178:333–340
- Gupta VK, Ali I (2004) Removal of lead and chromium from wastewater using bagasse fly ash—a sugar industry waste. *J Colloid Interface Sci* 271:321–328
- Gupta VK, Ali I (2008) Removal of endosulfan and methoxychlor from water on carbon slurry. *Environ Sci Technol* 42:766–770
- Gupta VK, Rastogi A (2008a) Equilibrium and kinetic modeling of cadmium (II) biosorption by nonliving algal biomass *Oedogonium* sp. from aqueous phase. *J Hazard Mater* 153:759–766
- Gupta VK, Rastogi A (2008b) Sorption and desorption studies of chromium (VI) from nonviable cyanobacterium *Nostoc muscorum* biomass. *J Hazard Mater* 154:347–354
- Gupta VK, Rastogi A (2008c) Biosorption of lead from aqueous solutions by green algae *Spirogyra* species: equilibrium and adsorption kinetics. *J Hazard Mater* 152:407–414
- Gupta VK, Rastogi A (2008d) Biosorption of lead from aqueous solutions by non-living algal biomass *Oedogonium* sp. and *Nostoc* sp.—a comparative study. *Colloids Surf B* 64:170–178
- Gupta VK, Rastogi A (2009) Biosorption of hexavalent chromium by raw and acid-treated green alga *Oedogonium hatei* from aqueous solutions. *J Hazard Mater* 163:396–402
- Gupta VK, Rastogi A (2010) Adsorption studies on the removal of hexavalent chromium from aqueous solution using a low cost fertilizer industry waste material. *J Colloid Interface Sci* 342:135–141
- Gupta VK, Sharma S (2003) Removal of zinc from aqueous solutions using bagasse fly ash—a low cost adsorbent. *Ind Eng Chem Res* 42:6619–6624
- Gupta VK, Suhas A (2009) Application of low cost adsorbents for dye removal—a review. *J Environ Manage* 90:2313–2342
- Gupta VK, Rastogi A, Dwivedi MK, Mohan D (1997a) Process development for the removal of zinc and cadmium from wastewater using slag—a blast furnace waste material. *Sep Sci Technol* 32:2883–2912
- Gupta VK, Ali I, Saini VK (1997b) Adsorption studies on the removal of Vertigo Blue 49 and Orange DNA13 from aqueous solutions using carbon slurry developed from a waste material. *J Colloid Interface Sci* 315:87–93
- Gupta VK, Mohan D, Sharma S (1998) Removal of lead from wastewater using bagasse fly ash—a sugar industry waste material. *Sep Sci Technol* 33:1331–1343
- Gupta VK, Srivastava SK, Tyagi R (2000) Design parameters for the treatment of phenolic waste by carbon columns (obtained from fertilizer waste material). *Water Res* 34:1543–1550
- Gupta VK, Gupta M, Sharma S (2001) Process development for the removal of lead and chromium from aqueous solutions using red mud—an aluminum industry waste. *Water Res* 35:1125–1134
- Gupta VK, Mangla R, Agarwal S (2002) Pb (II) selective potentiometric sensor based on 4-tert-Butylcalix [4] arene in PVC matrix. *Electroanalysis* 14:1127–1132
- Gupta VK, Mittal A, Gajbe V, Mittal J (2006a) Removal and recovery of the hazardous azo dye acid orange 7 through adsorption over waste materials: bottom ash and de-oiled soya. *Ind Eng Chem Res* 45:1446–1453
- Gupta VK, Mittal A, Jain R, Mathur M, Sikarwar S (2006b) Adsorption of safranin-T from wastewater using waste materials—activated carbon and activated rice husk. *J Colloid Interface Sci* 303:80–86
- Gupta VK, Jain AK, Maheshwari G, Lang H (2006c) Copper (II)-selective potentiometric sensor based on porphyrins in PVC matrix. *Sensors Actuators B* 117:99–106
- Gupta VK, Mittal A, Kurup L, Mittal J (2006d) Adsorption of a hazardous dye, erythrosine, over hen feathers. *J Colloid Interface Sci* 304:52–57
- Gupta VK, Ali I, Saini VK (2007a) Defluoridation of wastewaters using waste carbon slurry. *Water Res* 41:3307–3316
- Gupta VK, Singh AK, Gupta B (2007b) Schiff bases as cadmium (II) selective ionophores in polymeric membrane electrodes. *Anal Chim Acta* 583:340–348
- Gupta VK, Jain R, Varshney S (2007c) Electrochemical removal of hazardous dye Reactofix Red 3 BFN from industrial effluents. *J Colloid Interface Sci* 312:292–296
- Gupta VK, Jain R, Mittal A, Mathur M, Shalini S (2007d) Photochemical degradation of the hazardous dye Safranin-T using TiO₂ catalyst. *J Colloid Interface Sci* 309:464–469
- Gupta VK, Jain R, Varshney S (2007e) Removal of Reactofix golden yellow 3RFN from aqueous solution using wheat husk—an agricultural waste. *J Hazard Mater* 142:443–448
- Gupta VK, Mittal A, Kurup L, Mittal J (2008) Adsorption of basic fuchsin using waste materials—bottom ash and de-oiled soya as adsorbents. *J Colloid Interface Sci* 319:30–39
- Gupta VK, Carrott PJM, Ribeiro Carrott MML, Suhas A (2009a) Low cost adsorbents: growing approach to wastewater treatment—a review. *Crit Rev Environ Sci Technol* 39:783–842

- Gupta VK, Goyal RN, Sharma RA (2009b) Comparative studies of neodymium (III)-selective PVC membrane sensors. *Anal Chim Acta* 647:66–71
- Gupta VK, Al Khayat M, Singh AK, Pal MK (2009c) Nano level detection of Cd(II) using poly(vinyl chloride) based membranes of Schiff bases. *Anal Chim Acta* 634:36–43
- Gupta VK, Goyal RN, Sharma RA (2009d) Novel PVC membrane based alizarin sensor and its application; Determination of vanadium, zirconium and molybdenum. *Int J Electrochem Sci* 4:156–172
- Gupta VK, Ali I, Saleh TA, Nayak A, Agarwal S (2012) Chemical treatment technologies for waste-water recycling—an overview. *RSC Adv*. doi:10.1039/C2RA20340E
- Ho YS, McKay G (1998) Sorption of dye from aqueous solution by peat. *J Chem Eng* 70:115–124
- Jain AK, Gupta VK, Sahoo BB, Singh LP (1995a) Copper (II)-selective electrodes based on macrocyclic compounds. *Anal Proc Incl Anal Commun (RSC)* 32:99–101
- Jain AK, Gupta VK, Singh LP (1995b) Neutral carrier and organic resin based membranes as sensors for uranyl ions. *Anal Proc Incl Anal Commun (RSC)* 32:263–265
- Jain AK, Gupta VK, Singh LP, Khurana U (1997a) Macrocyclic based membrane sensors for the determination of cobalt(II) ions. *Analyst* 122:583–586
- Jain AK, Gupta VK, Khurana U, Singh LP (1997b) A new membrane sensor for UO_2^{2+} , based on 2-hydroxyacetophenoneoxime-thiourea trioxane resin. *Electroanalysis* 9:857–860
- Langmuir I (1918) Adsorption of gases on plain surfaces of glass mica platinum. *J Am Chem Soc* 40:1316–1403
- McKay G, Blair HS, Gardener JR (1982) Adsorption of dyes on chitin. I. Equilibrium studies. *J Appl Polym Sci* 27:3043–3057
- Melnik L, Vysotskaja O, Kornilovich B (1999) Boron behavior during desalination of sea and underground water by electro dialysis. *Desalination* 124:125–130
- Mollah A, Schennach R, Parga JR, Cocke DL (2001) Electrocoagulation (EC)—science and applications. *J Hazard Mater* 84:29–41
- Mouedhen G, Feki M, De Petris WM, Ayedi HF (2008) Behaviour of aluminum electrodes in electrocoagulation. *J Hazard Mater* 150:124–135
- Nogawa K, Kobayashi E, Okubo Y, Suwazono Y (2004) Environmental cadmium exposure, adverse effects and preventive measure in Japan. *Biometals* 17:581–590
- Saleh TA, Gupta VK (2011) Column with CNT/magnesium oxide composite for lead(II) removal from water. *Environ Sci Pollut Res*. doi:10.1007/s11356-011-0670-6
- Sekar M, Sakthi V, Rengaraj S (2004) Kinetics and equilibrium adsorption study of lead(II) onto activated carbon prepared from coconut shell. *J Colloid Interface Sci* 279:307–313
- Sharma A, Bhattacharyya KG (2004) Adsorption of chromium(VI) on *Azadirachta indica* (neem) leaf powder. *Adsorption* 10:327–338
- Srivastava SK, Gupta VK, Dwivedi MK, Jain S (1995) Caesium PVC-crown (dibenzo-24-crown-8) based membrane sensor. *Anal Proc Incl Anal Commun (RSC)* 32:21–23
- Srivastava SK, Gupta VK, Mohan D (1997) Removal of lead and chromium by activated slag—a blast-furnace waste. *J Environ Eng* 123:461–468
- Vasudevan S, Lakshmi J (2011) Effects of alternating and direct current in electrocoagulation process on the removal of cadmium from water. *Sep Purif Technol* 80:643–651
- Vasudevan S, Lakshmi J (2012a) The adsorption of phosphate by graphene from aqueous solution. *RSC Adv*. doi:10.1039/C2RA20270K
- Vasudevan S, Lakshmi J (2012b) Effect of alternating and direct current in an electrocoagulation process on the removal of cadmium from water. *Water Sci Technol* 65:353–360
- Vasudevan S, Sozhan G, Ravichandran S, Jayaraj J, Lakshmi J, Margrat Sheela S (2008) Studies on the removal of phosphate from drinking water by electrocoagulation process. *Ind Eng Chem Res* 47:2018–2023
- Vasudevan S, Lakshmi J, Sozhan G (2009) Studies on the removal of iron from drinking water by electrocoagulation—a clean process. *Clean* 37:45–51
- Vasudevan S, Lakshmi J, Packiyam M (2010a) Electrocoagulation studies on removal of cadmium using magnesium electrode. *J Appl Electrochem* 40:2023–2032
- Vasudevan S, Lakshmi J, Vanathi R (2010b) Electrochemical coagulation for chromium removal: process optimization, kinetics, isotherm and sludge characterization. *Clean* 38:9–16
- Vasudevan S, Margrat Sheela S, Lakshmi J, Sozhan G (2010c) Optimization of the process parameters for the removal of boron from drinking water by electrocoagulation—a clean technology. *J Chem Technol Biotechnol* 85:926–933
- Vasudevan S, Lakshmi J, Sozhan G (2010d) Studies relating to removal of arsenate by electrochemical coagulation optimization, kinetics, coagulant characterization. *Sep Sci Technol* 45:1313–1325
- Vasudevan S, Lakshmi J, Sozhan G (2010e) Studies on the removal of arsenate by electrochemical coagulation using aluminium alloy anode. *Clean* 38:506–515
- Wang XK, Chen CL, Hu WP, Ding AP, Xu D, Zhou X (2005) Sorption of 243Am(III) to multi-wall carbon nanotubes. *Environ Sci Technol* 39:2856–2860
- WHO (2004) Manganese in drinking water. Background document for development of WHO guidelines for drinking water quality report
- Yang K, Wang X, Zhu L, Xing B (2006) Competitive sorption of pyrene, phenanthrene, and naphthalene on multiwalled carbon nanotubes. *Environ Sci Technol* 40:5804–5810
- Youssef AM, Nabarawuy TE, Samra SE (2004) Sorption properties chemically activated carbons I. Sorption of cadmium(II) ions. *Colloids Surf Physicochem Eng Asp* 235:153–163